Manganese−Bipyridine Complex Incorporated into Mesoporous MCM-41 Molecular Sieves

Zhaohua Luan, Jie Xu, and Larry Kevan*

Department of Chemistry, University of Houston, Houston, Texas 77204-5641

Received June 26, 1998. Revised Manuscript Received August 27, 1998

Siliceous (SiMCM-41) and aluminosilicate mesoporous molecular sieves (AlMCM-41) with variable framework Si/Al ratios have been used as supports to immobilize manganese 2,2′-bipyridine (L) complex cations, $[MnL_2]^{2+}$, via incipient-wetness impregnation or ion exchange with $MnL_2(NO_3)_2$ in acetonitrile. Electron spin resonance (ESR), diffuse reflectance ultraviolet−visible (UV−vis), and Fourier transform infrared (FTIR) spectroscopies, thermal gravimetric (TG) analysis, and electron probe microanalysis have been employed to investigate the chemical environment of manganese in these materials and its transformation with oxidation−reduction treatments. $[MnL_2]^{2+}$ cation loading by impregnation is quantitatively controllable. At low loadings corresponding to Mn/Si ratios less than 2.4×10^{-3} for AlMCM-41 with Si/Al = 30.4, the Mn^{2+} complex cations are monatomically dispersed with a sextet ESR signal at $g = 2.00$ and 95 G hyperfine coupling. They have a low thermal decomposition temperature of about 160 °C. With increasing loading, the Mn^{2+} complexes interact as indicated by loss of resolution of the ESR sextet of Mn^{2+}. The thermal decomposition temperature increases to 215−265 °C which is still lower than 307 °C for $MnL_2(NO_3)_2$ crystals. For impregnation with washing by acetonitrile, the Mn^{2+} complex cation loading approaches a maximum of Mn/Si = 5.7×10^{-3} for AlMCM-41 with Si/Al = 30.4. By ion exchange, a comparable maximum manganese complex loading of Mn/Si = 6.6×10^{-3} is reached for the same sample. For this ion-exchanged AlMCM-41 the ESR shows a strong singlet at $g = 2.00$ with 132 G line width which overlaps a poorly resolved Mn^{2+} sextet at $g = 2.00$. This 132 G wide line is assigned to Mn^{4+} complex cations. TG analysis shows that this Mn^{4+} complex cation is stable to 225 °C. The ion exchange capacity of AlMCM-41 is enhanced by increasing the framework aluminum content. SiMCM-41 shows some ion exchange capacity due to silanol groups. FTIR suggests that the immobilized Mn^{2+} complex cations maintain a cis-bipyridyl molecular configuration as in solution, and UV−vis shows a lower charge-transfer energy at 510 nm in comparison with 380 nm for $MnL_2(NO_3)_2$ microcrystals. This is consistent with the absence of nitrate ligands in the coordination sphere of the Mn^{2+} on the MCM-41 wall surfaces. Upon oxidation with hydrogen peroxide in acetonitrile, the ESR signal of the immobilized Mn^{2+} complex cations disappears and the ESR siginal of Mn^{4+} complex cations increases while the total spin concentration remains constant. This change is reversed by reduction by oxalic acid in acetonitrile. This suggests that immobilized manganese complex cations may serve as effective active sites for oxidation−reduction reactions at low temperature.

Introduction

Microporous aluminosilicate molecular sieves known as zeolites contain regular arrays of uniformly sized channels and admit molecules below a certain critical size into their extensive internal space, making them of interest as heterogeneous catalysts and sorbents.[1] For many catalytic applications, these zeolite materials have to be modified by incorporating various transition-metal ions into the aluminosilicate framework to create suitable acid sites or oxidation−reduction sites for target organic reactions.[2,3] This demand has greatly stimulated the development of various molecular sieve framework substitution technologies in the last three decades. A large volume of novel transition-metal ion substituted molecular sieve materials have been prepared and successfully used as catalysts, particularly for small molecule transformations.[3−5]

Processing large organic molecules requires a molecular sieve with larger pore size than that of conventional zeolites of less than 15 Å. This is satisfied with tubular aluminosilicate MCM-41 material which possesses uniform mesopore channels varying from about 15 Å to about 100 Å with a large internal surface area up to

(1) Clifton, R. A. *Inf. Circ.-U. S. Bur. Mines* **1987**, *IC9140*, 22.
(2) Feast, S.; Lercher, J. A. In *Recent Advances and New Horizons in Zeolite Science and Technology*; Chon, H., Woo, S. I., Park, S.-E., Eds.; Elsevier: Amsterdam, The Netherlands, 1996; Studies in Surface Science and Catalysis, Vol. 102, pp 363−412.
(3) Bellussi, G.; Rigutto, M. S. In *Advanced Zeolite Science and Applications*; Jansen, J. C., Stöcker, M., Karge, H. G., Weitkamp, J., Eds.; Elsevier: Amsterdam, 1994; Studies in Surface Science and Catalysis, Vol. 85, pp 177−213.
(4) Taramasso, M.; Perego, G., Notari, B. U.S. Pat. 4 410 501, 1983.
(5) Corma, A.; Iglesias, M.; Sánchez, F. *J. Chem. Soc., Chem. Commun.* **1995**, 1635.

10.1021/cm980453r CCC: $15.00
Published on Web 10/10/1998

1000 m^2/g.[6] A recent report shows that the channels of tubular aluminosilicate materials can be further expanded to about 300 Å.[7] Considerable effort has also been devoted to incorporating various transition-metal ions into the MCM-41 framework to tune its catalytic properties.[8−11]

Transition-metal ion modified zeolites are conventionally used as high-temperature catalysts for the transformation of small organic molecules at typical reaction temperatures of 300−600 °C.[12,13] Such high temperatures are required to create active sites and maintain their activity during reaction. Small molecule substrates and products are often thermally stable enough to survive these conditions. However, large molecules are less thermally stable and require milder reaction conditions. This might be achieved by introducing sites active at *low temperature* into MCM-41 channels.

Preliminary studies have shown that organometallic complexes of variable valence transition-metal ions (such as manganese, iron, cobalt, or copper) with strong ligands (such as bipyridyl, porphyrin, or phenanthroline) possess exceptional catalytic activity for selective oxidation reactions in homogeneous systems.[14,15] Immobilization of such transition-metal ion complexes in the channels of porous solids offers the possibility of achieving catalytic sites active at low temperature.[16−21] Immobilization of complex cations of Mn^{2+} with 2,2′-bipyridine (L) ligands has been previously achieved in the supercages of zeolite X and Y.[20] These functionalized zeolite materials can catalyze selective epoxidation of alkenes and give higher yield than other solid catalysts such as microporous titanosilicate TS-1 molecular sieves. However, immobilization in zeolites requires multistep "ship-in-a-bottle" synthesis, wherein Mn^{2+} is first ion exchanged into the zeolite in an aqueous solution followed by addition of the 2,2′-bipyridine ligand. In addition, X and Y zeolite channels constructed of 13 Å supercages linked with 7 Å windows are almost blocked by Mn^{2+} complex cations of about 12 Å. This limits the access of substrates into the zeolite and limits the reaction efficiency for the oxidation of organic compounds. Immobilization of Mn^{2+} complex cations in mesoporous aluminosilicate MCM-41 molecular sieve materials was recently shown by direct ion exchange of $MnL_2(NO_3)_2$ in acetonitrile.[21] The functionalized MCM-41 materials exhibited higher catalytic activity for the oxidation of styrene than the corresponding homogeneous catalyst and showed no significant loss of catalytic activity when recycled. However, this work did not fully characterize the catalytically active manganese site.

In the present work, manganese 2,2′-bipyridine complex cations, $[MnL_2]^{2+}$, have been incorporated into siliceous (SiMCM-41) and aluminosilicate mesoporous molecular sieves (AlMCM-41) with variable Si/Al ratios via incipient-wetness impregnation or ion exchange in acetonitrile. Systematic study by electron spin resonance (ESR), diffuse reflectance ultraviolet−visible (UV−vis), and Fourier-transform infrared (FTIR) spectroscopies, thermogravimetric (TG) analysis, and electron probe microanalysis (EPMA) elucidates the chemical environment of the manganese in these materials and its transformation under oxidation−reduction conditions.

Experimental Section

Sample Preparation. A detailed synthesis procedure for siliceous MCM-41 and aluminosilicate AlMCM-41 with only tetrahedral framework aluminum has been described.[22,23] The white solid products, designated as SiMCM-41 or AlMCM-41-(X) where X is the Si/Al ratio by electron probe microanalysis, were calcined in static air at 550 °C for 24 h to decompose the organic structure-directing agent and used as manganese complex supports. Manganese 2,2′-bipyridine complex nitrate $MnL_2(NO_3)_2$ was prepared following a literature report.[24] A solution of 2,2′-bipyridyl and manganese nitrate (both from Aldrich) in ethanol, after standing at room temperature for about 30 min, yielded yellow crystals of $MnL_2(NO_3)_2$.

Manganese complex cations were loaded onto the supports at room temperature by incipient-wetness impregnation or ion exchange. Loading by impregnation was performed by adding 10 wt % MCM-41 powder to 90 wt % dimethylformamide/acetonitrile (1:9 v/v) containing dissolved $MnL_2(NO_3)_2$ followed by evaporation. The $MnL_2(NO_3)_2$ concentration varies from 0.0001 to 0.0700 M depending on the desired manganese complex loading. Impregnated samples were either not washed or were vigorously washed with acetonitrile, dried in a vacuum, and stored in a vacuum at room temperature. Loading by liquid-state ion exchange was done in nitrogen or in air at room temperature by stirring MCM-41 powder in 0.0204 M $MnL_2(NO_3)_2$ in acetonitrile for varying times up to 3 days. The ion-exchanged samples were filtered, washed with acetonitrile, and then dried in a vacuum and stored in a vacuum. These samples are described as MnL-SiMCM-41 or MnL-AlMCM-41-(X).

Oxidation−Reduction Treatment. Room-temperature oxidation was carried out in 5 mL of aqueous hydrogen peroxide (30 wt %)/acetonitrile solution (1:10 v/v) into which 100 mg of MnL-SiMCM-41 or MnL-

(6) Kresge, C. T.; Leonowicz, M. E.; Roth, W. J.; Vartuli, J. C.; Beck, J. S. *Nature* **1992**, *359*, 710.
(7) Zhao, D.; Feng, J.; Huo, Q.; Melosh, N.; Fredrickson, G. H.; Chmelka, B. F.; Stucky, G. D. *Science* **1998**, *279*, 548.
(8) Sayari, A. *Chem. Mater.* **1996**, *8*, 1840.
(9) Thomas, J. M.; Greaves, G. N. *Science* **1994**, *265*, 1675.
(10) Morey, M.; Davidson, A.; Eckert, H.; Stucky, G. *Chem. Mater.* **1996**, *8*, 486.
(11) Tuel, A.; Gontier, S. *Chem. Mater.* **1996**, *8*, 114.
(12) Magee, J. S.; Cormier, W. E.; Woltermann, G. M. *Oil Gas J.* **1985**, *83*, 59.
(13) Corma, A.; Martinez, A.; Martinez-Soria, V.; Monton, J. B. *J. Catal.* **1995**, *153*, 25.
(14) Meunier, B. *Chem. Rev.* **1992**, *92*, 1411.
(15) Jørgensen, K. A. *Chem. Rev.* **1989**, *89*, 431.
(16) Ozin, G. A.; Ozkar, S. *Chem. Mater.* **1992**, *4*, 511.
(17) Nakamura, M.; Tatsumi, T.; Tominaga, H. *Bull. Chem. Soc. Jpn.* **1990**, *63*, 3334.
(18) Herron, N. *J. Coord. Chem.* **1988**, *19*, 25.
(19) Liu, C. J.; Li. S. G.; Pang, W. Q.; Che, C. M. *J. Chem. Soc., Chem. Commun.* **1997**, 65.
(20) Knops-Gerrlts, P.-P.; Vos, D. D.; Thlbault-Starzyk, F.; Jacobs, P. A. *Nature* **1994**, *369*, 543.
(21) Kim, S.-S.; Zhang, W.; Pinnavaia, T. J. *Catal. Lett.* **1997**, *43*, 149.
(22) Luan, Z.; Cheng, C.-F.; Zhou, W.; Klinowski, J. *J. Phys. Chem.* **1995**, *99*, 1018.
(23) Luan, Z.; He, H.; Zhou, W.; Cheng, C.-F.; Klinowski, J. *J. Chem. Soc., Faraday Trans.* **1995**, *99*, 2955.
(24) Addison, C. C.; Kilner, M. *J. Chem. Soc., Chem. Commun.* **1966**, 1249.

Table 1. Elemental Compositions by EPMA and Pore Structure Parameters[23] of the Support Materials

samples	Si/Al ratio	surface area (m^2/g)	pore diameter (Å)
SiMCM-41		1263	30.0
AlMCM-41-(69.9)	69.9		
AlMCM-41-(30.4)	30.4	990	30.0
AlMCM-41-(9.8)	9.8		

AlMCM-41-(X) was added. The slurry mixture was stirred for 4 h, filtered, washed with acetonitrile, dried in a vacuum, and stored in a vacuum. Room temperature reduction was performed in 0.01 M oxalic acid in acetonitrile and was similarly processed.

Characterization. The elemental composition of the resultant solid products was analyzed by EMPA using a JEOL JXA-8600 spectrometer.

FTIR measurements were performed on a Nicolet 740 FTIR spectrometer using self-supported KBr pellets. The pellets contained about 1 wt % of finely powdered sample and were pressed at 4 tons/cm^2.

For ESR measurements, samples were loaded into 3 mm o.d. by 2 mm i.d. Suprasil quartz tubes. ESR spectra were recorded at X-band at either 293 or 77 K on a Bruker ESP 300 spectrometer. The magnetic field was calibrated with a Varian E-500 gaussmeter. The microwave frequency was measured by a Hewlett-Packard HP 5342A frequency counter.

UV−vis spectra were measured with a Perkin-Elmer 330 spectrophotometer equipped with a 60 mm Hitachi integrating sphere accessory. Powder samples were loaded in a quartz cell with Suprasil windows and spectra were collected in the 200−1000 nm wavelength range against a SiMCM-41 standard.

Thermal analysis was carried out on a Dupont 9900 thermal analyzer in nitrogen at a heating rate of 10 °C/min. The results were presented as thermogravimetric (TG) and differential thermogravimetric (DTG) curves.

Results

EPMA. Electron microprobe analysis shows that all MCM-41 supports and the resulting MnL-SiMCM-41 and MnL-AlMCM-41 materials have unique compositions and a homogeneous distribution of silicon, aluminum, and manganese complex over a particle. The framework Si/Al ratios of the MCM-41 supports are relatively close to those in the gel mixtures (Table 1) as previously analyzed by X-ray fluorescence spectroscopy.[22] The Mn/Si ratios of the MnL-SiMCM-41 and MnL-AlMCM-41 materials prepared via impregnation without washing agree with the amount of Mn^{2+} complex added to the impregnation soution. Materials prepared via impregnation with washing or by ion exchange show a maximum loading for the manganese complex dependent on the Si/Al ratios (Table 2).

Table 1 also gives the pore structure parameters of the support materials. The surface area is slightly decreased upon incorporation of framework aluminum, but the mesoporous structure is retained.[23] The MCM-41 pore diameter of about 30 Å along with an estimated 12 Å diameter for a manganese complex enables calculation of the manganese complex loading corresponding to filled channels which is Mn/Si = 35.0×10^{-3}.

FTIR. FTIR spectra of immobilized manganese complex cations in MCM-41 show only minor frequency shifts from those of the corresponding complex in solution (spectra not shown). It seems that the manganese complex maintains its original molecular configuration upon loading into MCM-41 materials.

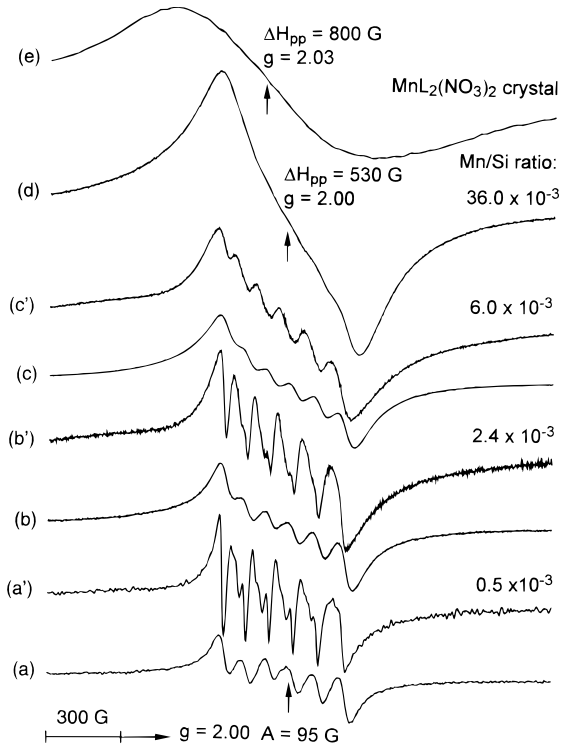

Figure 1. ESR spectra at 293 K of MnL-AlMCM-41-(30.4) prepared via impregnation without washing with Mn/Si ratios (a) 0.5×10^{-3}, (b) 2.4×10^{-3}, (c) 6.0×10^{-3}, (d) 36.0×10^{-3}, and (e) $MnL_2(NO_3)_2$ crystals. a′, b′, and c′ are ESR spectra at 77 K of the corresponding samples.

Table 2. Saturation Loadings by EPMA of Mangenese Bipyridine Complex on the Support Materials with Variable Framework Aluminum Content

	Mn/Si ratio	
samples	impregnation with washing	ion exchange
MnL-SiMCM-41	3.9×10^{-3}	4.6×10^{-3}
MnL-AlMCM-41-(69.9)		4.9×10^{-3}
MnL-AlMCM-41-(30.4)	5.7×10^{-3}	6.6×10^{-3}
MnL-AlMCM-41-(9.8)		8.2×10^{-3}

The solution spectra of trans-bipyridyl (lime-green) and cis-bipyridyl (yellow) manganese complexes show bands at 757 and 772 cm^{-1} for the cis form and a band at 765 cm^{-1} for the trans form.[24] Our manganese complex solution is yellow, and all manganese complex loaded samples give a broad band at 772 cm^{-1} which supports a cis-type manganese complex.

ESR. *Loading by Impregnation without Washing.* Figure 1 shows ESR spectra of manganese complexes in MnL-AlMCM-41-(30.4) prepared via impregnation without washing. At low manganese complex loading corresponding to a Mn/Si ratio less than 2.4×10^{-3}, the ESR spectra at 293 and 77 K show differences. At 293 K six well-resolved hyperfine lines centered at $g = 2.00$, originating from Mn^{2+} coupled to its own nuclear spin (^{55}Mn, $I_n = {}^5/_2$), are observed (Figure 1a,b). The sextet lines of Mn^{2+} are not equal in spacing and line height due to significant zero-field interaction.[25] An average hyperfine splitting constant of $A = 95$ G is obtained by

averaging the five separations between successive hyperfine lines. The *g*-value and hyperfine coupling constant are typical of Mn^{2+} in octahedral coordination as observed in several molecular sieves[25,26] and are so assigned here. At 77 K, in addition to the spectral features mentioned above, lines corresponding to forbidden transitions ($\Delta M = 1$, $\Delta m = 1$ transitions, where M is the electron spin quantum number and m is the nuclear spin quantum number) appear between the sextet lines of the allowed transitions (Figure 1a′,b′). The observation of forbidden transitions indicates that zero magnetic field interactions are not averaged by motion of the Mn^{2+} complex and support an immobile manganese complex at 77 K. Since no superimposed broad singlet from interacting Mn^{2+} is observed, these manganese complexes appear to be monatomically dispersed.

With increasing manganese complex loading, the ESR spectra at 293 and 77 K do not show much difference (Figure 1c,c′). The sextet lines slightly broaden and the lines corresponding to forbidden transitions become unobservable at 77 K (Figure 1b,c). This indicates increasing spin interaction between manganese species so there is a manganese complex loading above which the Mn^{2+} complexes are close enough to show detectable interaction. For MnL-AlMCM-41-(30.4), this loading corresponds to a Mn/Si = 2.4×10^{-3} for which the average separation betwen Mn^{2+} complexes is about 75 Å based on the measured suface area (Table 1). Since the interior surface is strongly curved, the actual separation is less.

Further increase in manganese complex loading to Mn/Si = 36.0×10^{-3} results in a broad singlet at $g = 2.0$ with overall peak-to-peak line width $\Delta H_{pp} = 530$ G (Figure 1d). For this loading the channels are filled. Additional manganese complex loading must occur on the external surface and the singlet ESR line width approaches that of $MnL_2(NO_3)_2$ microcrystals (Figure 1e).

Loading by Impregnation with Washing. A comparison of the ESR spectra at 293 K of a series of MnL-AlMCM-41 samples prepared via impregnation with and without washing by acetonitrile is given in Figure 2. This shows that upon washing the ESR intensity of MnL-AlMCM-41 materials decreases only slightly for manganese complex loading less than Mn/Si = 6.0×10^{-3} (Figure 2A,a−c and Figure 2B,a′−c′), but decreases much more at higher loading (Figure 2A,d and Figure 2B,d′). This is shown quantitatively by the doubly integrated ESR intensities in Figure 3. Above a manganese complex loading corresponding to Mn/Si = 5.7×10^{-3}, the loading plateaus for washed samples, while for unwashed samples the ESR intensity increases linearly. This indicates that impregnated AlMCM-41 with washing can only immobilize a maximum amount of manganese complexes. For MnL-AlMCM-41-(30.4) this corresponds to Mn/Si = 5.7×10^{-3}.

Loading by Ion Exchange. Room-temperature ESR spectra of a series MnL-AlMCM-41-(30.4) samples prepared via ion exchange with variable stirring times are shown in Figure 4. In contrast to impregnated samples,

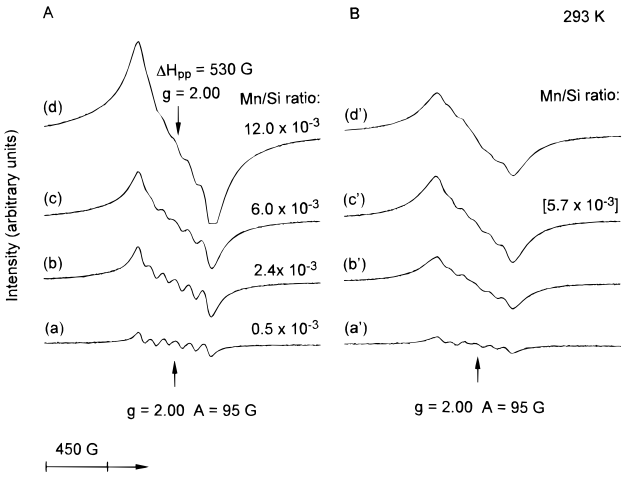

Figure 2. A comparison of ESR spectra at 293 K (on the same scale) of MnL-AlMCM-41-(30.4) prepared via impregnation (A) without and (B) with washing. The initial manganese complex loadings correspond to Mn/Si ratios (a, a′) 0.5×10^{-3}, (b, b′) 2.4×10^{-3}, (c, c′) 6.0×10^{-3}, and (d, d′) 12.0×10^{-3}. The number in square brackets for a washed sample indicates analysis data by EPMA.

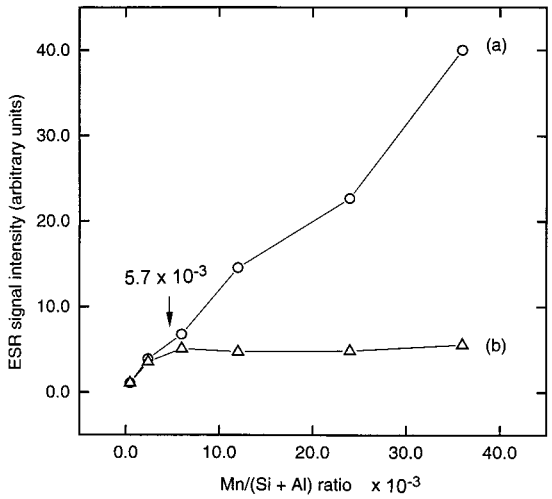

Figure 3. Plot of doubly integrated ESR intensity at 293 K of MnL-AlMCM-41-(30.4) prepared via impregnation (a) without and (b) with washing versus the initial manganese complex loading as Mn/(Si +Al).

different spectroscopic features are observed. In addition to the sextet lines (Figure 4a) a broad singlet is observed upon stirring (Figure 4b). This singlet develops more with increasing stirring time at the expense of the sextet lines and predominates at prolonged stirring time (Figure 4b−f). Note that the singlet is narrower than the overall splitting for Mn^{2+}. Subtraction of the isolated Mn^{2+} spectrum (sextet) from the spectra in Figure 4 yields spectra which show that the singlet can be characterized by $g = 2.00$ and $\Delta H_{pp} = 132$ G (Figure 4b′). Ion exchange of the manganese complex into AlMCM-41 was performed both in air and in N_2 but the ESR spectra were similar. The line width of this singlet is narrower than that of manganese complex crystals, and ion-exchanged samples have only a slightly higher maximum manganese complex content than impregnated samples with washing (Table 2). Therefore, assignment to a high local spin concentration of manganese complex can be ruled out. Since the singlet intensity can be greatly reduced upon reduction

(25) Xu, J.; Luan, Z.; Wasowicz, T.; Kevan, L. *Microporous Mesoporous Mater.* **1998**, *22*, 179.
(26) Goldfarb, D. *Zeolites* **1989**, *9*, 509.

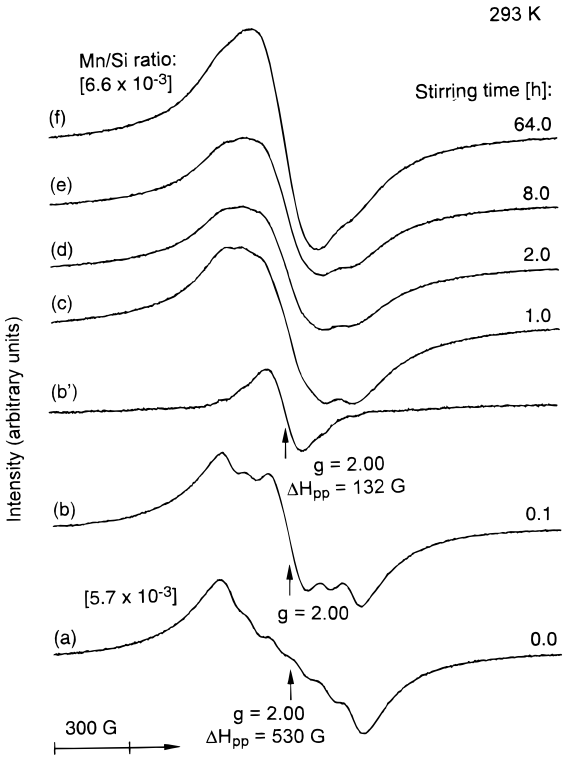

Figure 4. ESR spectra at 293 K (on the same scale) of MnL-AlMCM-41-(30.4) prepared via ion exchange with variable stirring time (a) 0.0, (b) 0.1, (c) 1.0, (d) 2.0, (e) 8.0, and (f) 64.0 h. Spectrum b′ shows spectrum b after subtraction of the spectrum without stirring. The numbers in square brackets indicate analysis data by EPMA.

by oxalic acid in acetonitrile and since the singlet also occurs in impregnated samples with washing that are oxidized by H_2O_2 in acetonitrile (see below), we assign this line to Mn^{4+} complex cations.

Oxidation−Reduction Treatment. The oxidation−reduction behavior of MnL-AlMCM-41 prepared via impregnation was studied with aqueous H_2O_2 (30 wt %) as oxidant in acetonitrile and with oxalic acid as reductant in acetonitrile. At manganese complex loading below Mn/Si = 2.4×10^{-3} (Figure 5A), oxidation produces an ESR singlet at $g = 2.00$ with $\Delta H_{pp} = 132$ G (Figure 5A,a2). This line is similar to that from ion-exchanged samples (Figure 4b′). Subsequent reduction converts the singlet to the sextet of isolated Mn^{2+} (Figure 5A,a3,a3′). Double integration of the ESR intensity shows no significant change in spin concentration. Mn^{3+} is ESR silent at conventional microwave frequencies (X-band, ∼9 GHz; Q-band, ∼35 GHz), while a recent report shows that it can be detected by high-frequency ESR spectroscopy (>90 GHz) in a manganese porphyrin system.[27] Our ESR spectra were measured at X-band where Mn^{3+} is not observable. Thus, the constant spin concentration and reversible spectral change in the course of oxidation−reduction treatments seems consistent with conversion between Mn^{2+} and Mn^{4+}.

At a manganese complex loading of Mn/Si = 5.7×10^{-3} (Figure 5B), the same ESR spectral change occurs upon oxidation (Figure 5B,b1,b2), but reduction does not totally reverse the spectrum even at prolonged reaction time (Figure 5B,b3). This contrasts with a manganese complex loading of Mn/Si = 2.4×10^{-3}, for which the Mn^{2+} complexes are isolated from one another and complete reduction does occur.

(27) Goldberg, D. P.; Telser, J.; Krzystek, J.; Montalban, A. G.; Brunel, L. C.; Barret, A. G. M.; Hoffman, B. M. *J. Am. Chem. Soc.* **1997,** *119,* 8722.

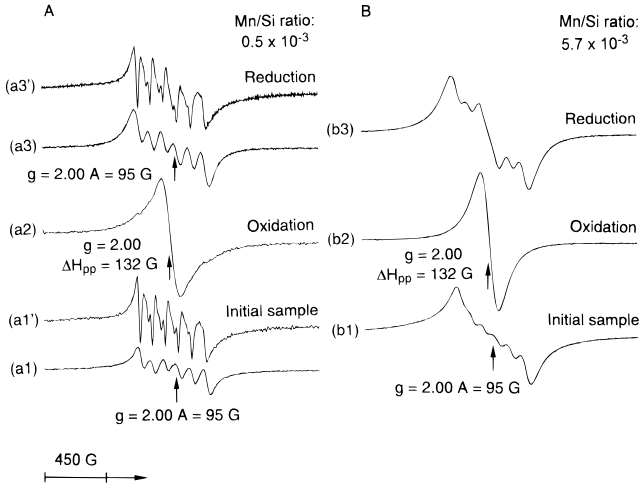

Figure 5. ESR spectra at 293 K of MnL-AlMCM-41-(30.4) prepared via impregnation with washing for Mn/Si ratios (A) 0.5×10^{-3} and (B) 5.7×10^{-3} for (a1, b1) initial sample and after (a2, b2) oxidation by H_2O_2 and (a3, b3) reduction by oxalic acid. a1′ and a3′ are ESR spectra at 77 K corresponding to spectra a1 and a3.

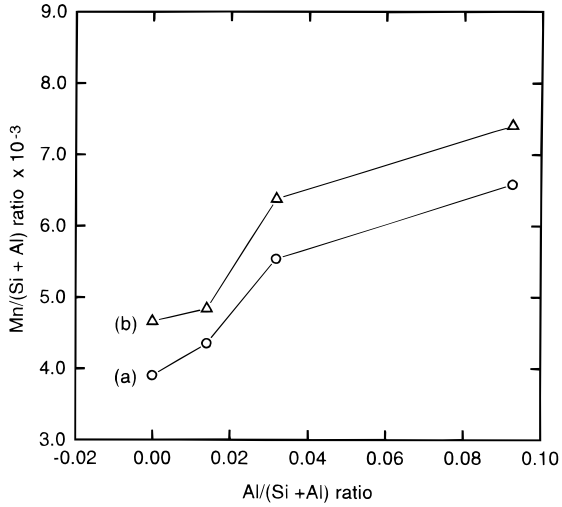

Figure 6. Dependence of saturation manganese complex loading upon the tetrahedral framework aluminum content for (a) ion-exchanged samples and (b) impregnated samples with washing.

Effect of Framework Si/Al Ratio on Manganese Complex Loading. The spectra from impregnated MnL-SiMCM-41 with washing are almost the same as those from MnL-AlMCM-41 except for lower manganese complex loading for MnL-SiMCM-41. For ion-exchanged MnL-SiMCM-41 an ESR singlet is only visible as a shoulder which broadens the sextet lines of the Mn^{2+} complex (spectra not shown). This contrasts with ion-exchanged MnL-AlMCM-41. This is probably due to lower manganese complex loading for MnL-SiMCM-41 than that for MnL-AlMCM-41 and thus less interaction between manganese complexes.

Figure 6 shows plots of the manganese complex loading as a function of the framework aluminum content [Al/(Si + Al)] for MnL-SiMCM-41 and MnL-

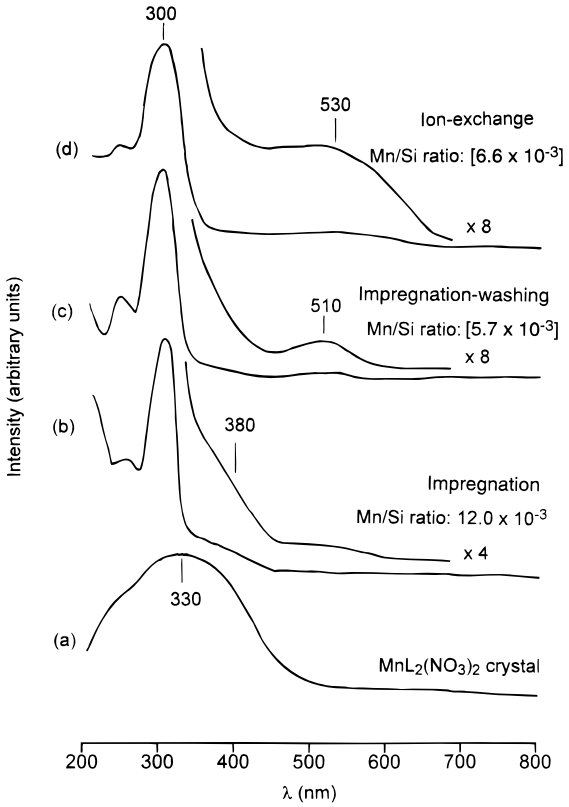

Figure 7. Diffuse reflectance UV−vis spectra of (a) $MnL_2(NO_3)_2$ crystals, (b) MnL-AlMCM-41-(30.4) with Mn/Si of 12.0×10^{-3} prepared via impregnation without washing, (c) the same sample as b with washing, and (d) MnL-AlMCM-41-(30.4) prepared via ion exchange with 64 h of stirring. The numbers in square brackets indicate analysis by EPMA.

AlMCM-41. The maximum manganese complex loading by either impregnation with washing or by ion exchange increases with increasing framework aluminum content. SiMCM-41 also shows significant ion exchange capacity up to Mn/Si = 4.6×10^{-3}. Silanol groups on SiMCM-41[23] serve as ion exchange sites.

UV−Vis. Figure 7 shows UV−vis spectra of various preparations of MnL-AlMCM-41-(30.4). $MnL_2(NO_3)_2$ microcrystals are yellow and have a broad band near 330 nm (Figure 7a). Upon loading into MCM-41 this band is separated into two bands at 300 and 380 nm (Figure 7b) which are assigned to charge-transfer transitions. Such charge-transfer transitions are typical for transition-metal complexes and transition-metal ion substituted zeolite materials.[3,5,10]

Impregnated AlMCM-41 with washing is pink instead of light yellow before washing or yellow for $MnL_2(NO_3)_2$ crystals. This color change is consistent with the absence of nitrate ligands in the coordination sphere of the manganese and indicates anchoring of the Mn^{2+} complex cations to the internal walls of AlMCM-41.[20,21] The UV−vis spectrum of light pink MnL-MCM-41-(30.4) shows a band at 510 nm instead of one at 380 nm (Figure 7c). Since this band is not observed in AlMCM-41 or $MnL_2(NO_3)_2$ microcrystals, this band is assigned to a metal-to-ligand charge-transfer transition of manganese complex cations bonded to MCM-41 wall surfaces.[17,20,21] The UV−vis spectrum of ion-exchanged MnL-AlMCM-41-(30.4) shows similar spectral features, but the band near 510 nm broadens toward lower energy (Figure 7d).

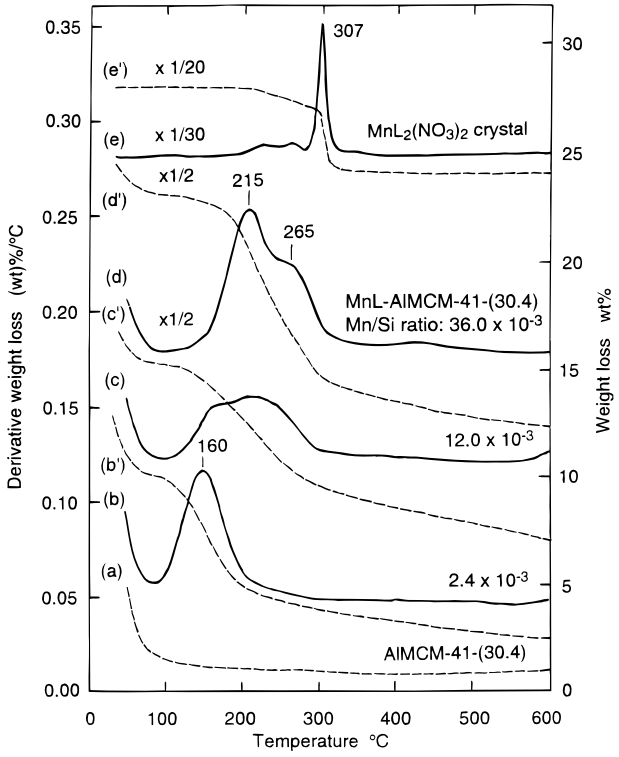

Figure 8. TG (dotted lines) and DTG curves (solid lines) of MnL-AlMCM-41-(30.4) prepared via impregnation without washing with Mn/Si ratios (a) 0, (b) 2.4×10^{-3}, (c) 12.0×10^{-3}, (d) 36.0×10^{-3}, and (e) $MnL_2(NO_3)_2$ crystals.

TG/DTG. Thermogravimetric analysis of a series of MnL-AlMCM-41 samples prepared via impregnation without washing are shown in Figure 8. The TG curves show that the total weight loss is associated with the manganese complex content corresponding to decomposition of the organic ligands (Figure 8b′−e′). When the manganese complex loading is below Mn/Si = 2.4×10^{-3} for AlMCM-41-(30.4), DTG shows that decomposition of organic ligands takes place at 160 °C (Figure 8b). As the manganese loading increases, the decomposition temperature increases to 215−265 °C (Figure 8c). As the manganese complex loading reaches Si/Al = 36.0×10^{-3}, the decomposition still occurs at 215−265 °C (Figure 8d). $MnL_2(NO_3)_2$ crystals decompose at 307 °C (Figure 8e). Since ESR suggests that the manganese complexes are present as isolated species at loadings below Mn/Si = 2.4×10^{-3}, it appears that increasing dispersion of the manganese complex results in lower thermal stability.

Figure 9 shows thermogravimetric analysis data for MnL-AlMCM-41 with maximum manganese complex loading by impregnation with washing and by ion exchange. All TG curves broaden toward higher decomposition temperature beyond 500 °C. The DTG curve from MnL-AlMCM-41 prepared via impregnation with washing shows a decomposition temperature at 180 °C (Figure 9a) which compares with 160 °C for an unwashed sample with low loading (Figure 9b). In contrast, ion-exchanged MnL-AlMCM-41 shows a higher thermal decomposition temperature at 225 °C (Figure 9b). Because ESR indicates oxidation of Mn^{2+} to Mn^{4+} complex cations for prolonged stirring, the TG result suggests a higher thermal stability for Mn^{4+} complex cations compared to Mn^{2+} complex cations on MCM-41

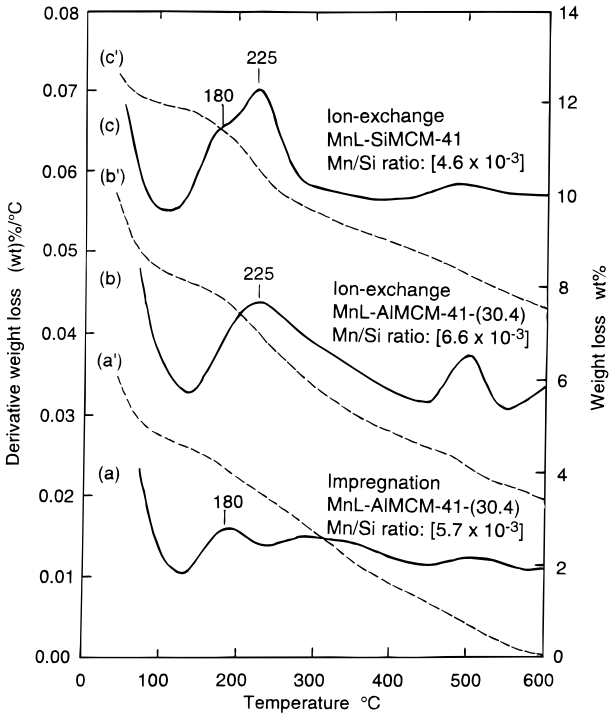

Figure 9. TG (dotted lines) and DTG curves (solid lines) of (a) MnL-AlMCM-41-(30.4) prepared via impregnation with washing, (b) MnL-AlMCM-41-(30.4) prepared via ion exchange with 64 h of stirring, and (c) MnL-SiMCM-41 prepared via ion exchange. The numbers in square brackets indicate analysis by EPMA.

surfaces. MnL-SiMCM-41 prepared via ion exchange exhibits two thermal decompositions at 180 and 225 °C, indicating the presence of both Mn^{2+} and Mn^{4+} complex cations. This is consistent with the ESR results.

Discussion

In addition to direct ion exchange,[21] incipient-wetness impregnation is effective for immobilization of manganese complex cations into mesoporous MCM-41 molecular sieve. Impregnation allows better control of the manganese complex loading.

Loading of Manganese Complex Cations onto MCM-41 Supports. For MnL-AlMCM-41 with Si/Al = 30.4 prepared via impregnation, ESR shows that for a manganese complex loading corresponding to Mn/Si = 2.4×10^{-3} and below there is monatomic dispersion of noninteracting manganese complexes. TG and DTG show that these isolated manganese complex cations are thermally stable up to 160 °C. The manganese complex loading by impregnation without washing can be increased to Mn/Si = 36.0×10^{-3} without formation of $MnL_2(NO_3)_2$ microcrystals. However with washing, the maximum manganese complex loading is only Mn/Si = 5.7×10^{-3}. A slightly higher maximum loading of Mn/Si = 6.6×10^{-3} is achieved by ion exchange. At these maximum loadings the manganese complexes interact and broaden the ESR lines.

For MnL-AlMCM-41-(30.4) prepared via impregnation with washing, each Mn^{2+} complex cation replaces two singly charged cations associated with tetrahedrally coordinated Al to maintain charge neutrality. A Mn/Si ratio of 5.7×10^{-3} for MnL-AlMCM-41-(30.4) corresponds to a Mn/Al ratio of 0.17. For doubly charged Mn^{2+} this accounts for about 34% of the aluminum sites. This is consistent with a recent study on AlMCM-41 which showed that about 40% of the aluminum sites are accessible for ion exchange.[28] The amount of immobilized manganese complex cations on AlMCM-41 is enhanced by increasing the framework aluminum content. SiMCM-41 also shows significant loading to Mn/Si = 4.6×10^{-3} indicating that silanol groups in SiMCM-41 also serve as ion exchange sites.

The Occurrence of Mn^{4+} Complex Cations. For impregnated MnL-AlMCM-41, ESR confirms the presence of Mn^{2+} complexes, but for ion-exchanged MnL-AlMCM-41, ESR shows a $g = 2.00$ singlet with $\Delta H_{pp} =$ 132 G which overlaps with the sextet lines of Mn^{2+}. The singlet intensity is reduced by oxalic acid and also occurs in impregnated samples after oxidation by H_2O_2. Thus, this singlet is assigned to Mn^{4+} complex cations.

Previous studies have shown that line width narrowing is observed when magnetic ions are less than 10−20 Å apart and the exchange interaction exceeds the dipole interaction.[29,30] Manganese-substituted AlPO-5 shows broadening of the Mn^{2+} sextet into a single line indicating an increase in the spin-exchange interaction.[26] The ESR spectra from Mn^{4+} species show a g-value slightly less than 2.0, whereas for Mn^{2+} it is slightly above 2.0. The hyperfine splitting ranges from 61 to 66 G for Mn^{4+} and from 70 to 95 G for Mn^{2+}.[25,31] The different spectroscopic parameters in the literature of immobilized Mn^{4+} cations in AlMCM-41 may be due to different coordination environments.

Redox Cycle of Immobilized Manganese Complex Cations. Upon oxidation by hydrogen peroxide in acetonitrile Mn^{2+} complex cations are completely converted to Mn^{4+} complex cations both at low and high manganese complex loadings. However for reduction by oxalic acid in acetonitrile, MnL-AlMCM-41 samples with variable manganese complex loading show differences in the amount of reduction. At low manganese complex loading, the ESR spectrum shows a resolved hyperfine sextet of isolated Mn^{2+} ions, indicating complete reduction of Mn^{4+} to Mn^{2+} species. Isolated manganese complex cations have a reversible redox cycle. The promotion effect of AlMCM-41 on the oxidation−reduction characteristics of immobilized manganese complex cations is apparently related to their dispersion. For maximum manganese complex loading, complete oxidation to Mn^{4+} complexes occurs but complete reduction does not occur even at prolonged reaction time.

The appearance of a UV−vis band around 510 nm from immobilized manganese complex cations instead of a band around 380 nm from manganese complexes in solution indicates a lower charge-transfer transition energy which supports transformation from Mn^{2+} to Mn^{4+}. This reversible Mn^{2+}/Mn^{4+} redox cycle suggests that manganese complex cations immobilized on MCM-41 materials may serve as active sites for oxidation−reduction reactions. For example, in the reaction mechanism proposed[14,15] for the homogeneous oxidation

(28) Luan, Z.; Xu, J.; Kevan, L. *Nukleonika* **1997**, *42*, 493.
(29) Abragam, A.; Bleaney, B. *Electron Paramagnetic Resonance of Transition Ions*; Oxford: Cambridge, 1970; p 58.
(30) McNally, J. M.; Kreilick, R. W. *J. Phys. Chem.* **1982**, *86*, 421.
(31) Kijlstra, W. S.; Poels, E. K.; Bliek, A.; Weckhuysen, B. M.; Schoonheydt, R. A. *J. Phys. Chem. B* **1997**, *101*, 309.

of olefins by Mn−porphyrin and related compounds, manganese complex cations are believed to form a high-valent species such as Mn^{4+}.

The difference in oxidation−reduction properties of manganese complex cations at variable loading may account for previous reaction data[21] in which samples with low manganese complex loading (Si/Al = 9, Mn/Si = 5.6×10^{-3}) showed higher activity than those with high loading (Si/Al = 9, Mn/Si = 7.8×10^{-3}). On the basis of our results, this can be interpreted as due to greater interaction of manganese complex cations at higher loading which gives lower activity. This also suggests that isolated manganese complexes are more active for catalytic reaction.

Conclusions

Manganese complex cations, $[MnL_2]^{2+}$, have been incorporated into mesoporous MCM-41 molecular sieves. A combination of ESR, UV−vis, and FTIR spectroscopies as well as thermogravimetric measurement has characterized the chemical environment of manganese in these materials. The results show that Mn^{2+} complex cation loading by impregnation followed by washing with acetonitrile is quantitatively controllable and has a maximum loading of Mn/Si = 5.7×10^{-3} for AlMCM-41 with Si/Al = 30.4. Comparable saturation manganese complex loading of Mn/Si = 6.6×10^{-3} is achieved for AlMCM-41 by ion exchange. The maximum manganese complex loading in AlMCM-41 is enhanced by increasing the framework aluminum content. SiMCM-41 also shows significant ion exchange capacity associated with its silanol groups. Upon oxidation by hydrogen peroxide in acetonitrile or reduction by oxalic acid in acetonitrile these immobilized manganese complex cations cycle between Mn^{2+} and Mn^{4+} complex cations. This redox transformation does not occur in solution. This suggests that the immobilized manganese complex cations may serve as catalytically active sites at low temperature for oxidation−reduction reactions in molecular sieves.

Acknowledgment. This research was supported by the Robert A. Welch Foundation, the University of Houston Energy Laboratory, and the National Science Foundation.

CM980453R